Chapter 2

Subcritical dynamo and bi-stability in large-scale kinematic dynamo model

We now know that the convective flow of the ionized plasma in the CZs of the Sun and Sun-like stars is responsible for the generation of the magnetic field and cycles through the hydromagnetic dynamo (Moffatt, 1978; Charbonneau, 2020). It is evident now that in the dynamo, differential rotation and helical convective flow play essential roles. This is because the differential rotation of the star generates the toroidal field from the poloidal one through the Ω effect, and the helical turbulence (α effect) &/or Babcock–Leighton process induces the poloidal field from the toroidal one.

In this type of α-Ω dynamo model, the governing parameter is the dynamo number, which is defined as,

$$\mathbf{D} = \frac{\alpha \Delta \Omega R^3}{\eta^2}, \tag{2.1}$$

where, α is the measure of α-effect, $\Delta\Omega$ is the variation in the angular velocity in the sun/star, R is its radius, and η is the turbulent magnetic diffusivity Krause & Rädler (1980). There is a critical dynamo number (D_c) below which the dynamo is not possible and the initial magnetic field decay. The regime below D_c is known as the subcritical regime and above D_c is called the supercritical regime (Choudhuri, 1998; Kumar et al., 2021).

[†]This chapter is based on Vashishth et al. (2021), *RAA*, 21, 10, 266.

Since the rotation rate of a star decreases with age (Skumanich, 1972; Rengarajan, 1984), the dynamo number D is expected to decrease as the star spins down (Kitchatinov & Nepomnyashchikh, 2017). Therefore, the question is, will the dynamo cease immediately when $D < D_c$?

2.1 Introduction

It has been found that the dynamo is still possible when $D < D_c$. Kitchatinov & Olemskoy (2010) have shown this subcritical dynamo in a kinematic mean-field dynamo model with non-linear quenching in α and η. They found that if the dynamo is started with a strong magnetic field in the subcritical regime, a strong oscillating dynamo solution is possible. In contrast, when the dynamo is initiated with a weak field, a decaying solution is produced. Thus this dependence of the magnetic field with the dynamo number shows a hysteresis behaviour. Further, in a simplified model, Kitchatinov & Nepomnyashchikh (2015) showed that transitions between two modes (subcritical dynamo with finite magnetic field and supercritical dynamo) qualitatively reproduce two distinct modes in the distribution of solar activity as inferred from cosmogenic isotope content in natural archives (Usoskin et al., 2014). This behavior was further supported by Karak et al. (2015b) in the turbulent dynamo simulations.

In the study mentioned above by Kitchatinov & Olemskoy (2010), a helical α, distributed over the whole CZ was used. However, recently, there are observational supports for the predominance of the Babcock–Leighton process for the generation of a poloidal field in the Sun (Dasi-Espuig et al., 2010; Kitchatinov & Olemskoy, 2011a; Muñoz-Jaramillo et al., 2013; Priyal et al., 2014; Cameron & Schüssler, 2015). Various surface flux transport (Wang et al., 1989; Baumann et al., 2004; Jiang et al., 2014a) and dynamo models (Karak et al., 2014a; Choudhuri, 2018; Charbonneau, 2020) based on this Babcock–Leighton process alone have been successful in modeling various aspects of solar magnetic fields and cycles. Therefore, in this study, we shall explore the subcritical dynamo in a Babcock–Leighton type solar dynamo model.

As our model is kinematic, we do not capture any nonlinearity in the mean flows. We,

however, consider magnetic field dependence nonlinearity in turbulent diffusivity and Babcock–Leighton α. While diffusivity quenching has been proposed in several theoretical studies and supported by certain approximation (Kitchatinov et al., 1994a; Karak et al., 2014c), the quenching in Babcock–Leighton α is less constrained. In the Babcock–Leighton process, a poloidal field is produced by the decay and the dispersal of tilted bipolar magnetic regions (BMRs). This tilt has some magnetic field dependence, although its exact dependence is not well constrained (Dasi-Espuig et al., 2010; Jha et al., 2020). There is also a latitudinal variation of BMRs with the solar cycle (Mandal et al., 2017) which may be a source of nonlinear quenching (Jiang, 2020; Karak, 2020). In our study, we shall consider magnetic field-dependent quenching in both diffusivity and α based on quasi-linear approximation as presented in Ruediger & Kichatinov (1993); Kitchatinov et al. (1994a).

In the Babcock–Leighton α, there is some inherent randomness as primarily seen in the tilts of BMRs around Joy's law (Dasi-Espuig et al., 2010; Stenflo & Kosovichev, 2012; McClintock et al., 2014; Wang et al., 2015; Arlt et al., 2016; Jha et al., 2020). These fluctuations can have a severe impact on the magnetic cycle and particularly on the existence of the subcritical dynamo branch. Therefore we shall also include the fluctuations in the Babcock–Leighton α term of our dynamo model and check the dynamo behavior in different regimes.

2.2 Model

For our study, we consider the magnetic field to be axisymmetric, and thus, we express it in the same manner as equations (1.13) and (1.12). In the classical $\alpha\Omega$ mean-field model, S is due to the helical nature of the convective flow. However, in the case of the Babcock–Leighton process, the poloidal field is generated near the surface through the decay and dispersal of tilted BMRs. In our axisymmetric model, this process has been routinely parameterized as

$$S(r, \theta; B) = \alpha_{\rm BL} \overline{B}(\theta, t), \tag{2.2}$$

where $\overline{B}(\theta, t)$ is the average toroidal field in a thin layer at the base of the CZ (BCZ) ($0.675R_s < r < 0.725R_s$) and $\alpha_{\rm BL}$ is the parameter for Babcock–Leighton process. We write,

$$\alpha_{\rm BL} = \alpha\phi_\alpha(\beta), \tag{2.3}$$

where $\beta = B/B_0$ with B_0 being the equipartition field strength. The α is the profile for the usual Babcock–Leighton α which has the following form:

$$\alpha = \frac{\alpha_0}{4}\left[1 + \text{erf}\left(\frac{r - 0.95R_\odot}{0.05R_\odot}\right)\right] \times \left[1 - \text{erf}\left(\frac{r - R_\odot}{0.01R_\odot}\right)\right] \frac{\sin\theta\cos\theta}{1 + \exp(K)}, \tag{2.4}$$

for $\theta < \pi/2$, $K = 30(\pi/4 - \theta)$ and for $\theta > \pi/2$, $K = 30(\theta - 3\pi/4)$. The $\phi_\alpha(\beta)$ in Eq. (2.3) has the following magnetic field dependent quenching based on quasi-linear approximation as presented in Ruediger & Kichatinov (1993).

$$\phi_\alpha(\beta) = \frac{15}{32\beta^4}\left[1 - \frac{4\beta^2}{3(1+\beta^2)^2} - \frac{1-\beta^2}{\beta}\arctan\beta\right]. \tag{2.5}$$

The turbulent diffusivity η_T has the following form.

$$\eta_T = \eta\phi_\eta(\beta), \tag{2.6}$$

where

$$\eta = \eta_0\left[\eta_{in} + \left(\frac{1-\eta_{in}}{2}\right)\left(1 + \text{erf}\left(\frac{r - x_n}{h_n}\right)\right)\right] \tag{2.7}$$

with $\eta_{in} = 10^{-4}$, $x_n = 0.70R_\odot$, $h_n = 0.05R_\odot$, $\eta_0 = 5 \times 10^{12} cms^2$. We consider a magnetic field dependent quenching in the diffusivity following Kitchatinov et al. (1994b)

$$\phi_\eta(\beta) = \frac{3}{8\beta^2}\left[1 + \frac{4 + 8\beta^2}{(1+\beta^2)^2} + \frac{\beta^2 - 5}{\beta}\arctan\beta\right]. \tag{2.8}$$

We note that both α and η_T are quenched through the local magnetic field. In section 2.3.2, however, we shall change this prescription and relate α and η_T through the magnetic field at the BCZ. The differential rotation Ω and the boundary conditions are the same as that used in Nandy & Choudhuri (2002); Chatterjee et al. (2004).

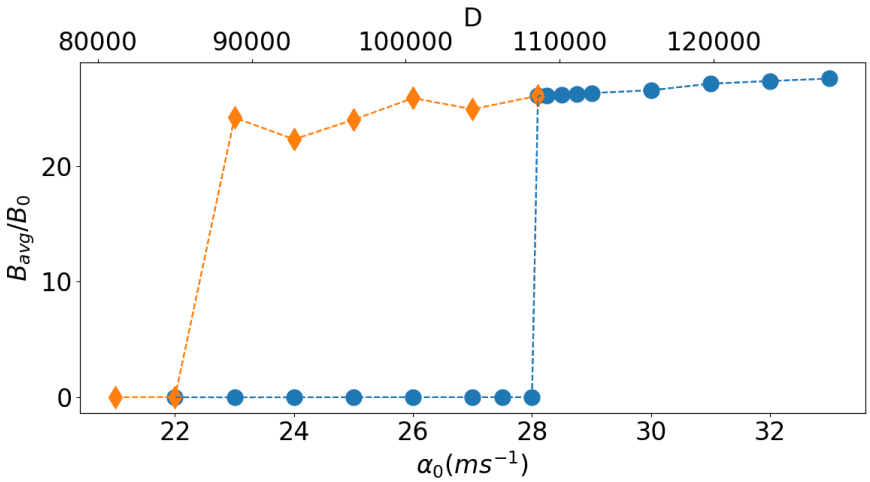

Figure 2.1: Dynamo hysteresis: Variation of the temporal average of the mean toroidal field normalized to B_0 and computed at the BCZ at latitude $-14°$ (B_{avg}) as a function of α_0 (in m s^{-1}) from simulations started with a weak field (filled circles) and from simulations started with strong field of previous simulation (orange diamonds). The corresponding D is shown in top horizontal axis.

2.3 Results

2.3.1 Quenching with the local field

By including the magnetic field dependent quenching in η_T and α and by specifying the large-scale flows, such as differential rotation and meridional circulation, we solve the dynamo equations (1.13) and (1.12). We first identify the dynamo transition. To do so, we perform simulations at different values of α_0, i.e., at different values of dynamo number, defined here as $D = \alpha_0 \Omega_0 R^3/\eta_0^2$ (where $\Omega_0 = 2\pi/T$; $T = 25.38$ days). We find that when we start the simulations with a very weak magnetic field, the initial magnetic field grows as long as $\alpha_0 \geq 28.10$ m s^{-1}. The dynamo number corresponding to this α_0, i.e., the critical dynamo number, $D_c = 1.086 \times 10^5$. The points connecting the solid line in Fig. 2.1 show $B_{\rm avg}$ versus α_0 and D. $B_{\rm avg}$ is computed at $0.7R_s$ and $-13°$ latitude and averaged over a few steady cycles. Now, instead of starting the simulation with a weak magnetic field, we start it with the output of an oscillatory solution of a strong magnetic field. We take the output of the simulation performed at $\alpha_0 = 28.10$ m s^{-1}and execute a new simulation at $\alpha_0 = 27$ m s^{-1}and then we take the output of this simulation and feed it into a new simulation at a lower α_0. In this way, we perform several simulations at a progressively lower α_0 by taking the output of the previous simulation at higher α_0.

The orange diamond points connecting the dotted line in Fig. 2.1 shows B_{avg} for these simulations. The interesting behaviour we observe is that the solutions are different than the ones performed at the same parameters but started with a weak field. We find a wide region in the dynamo parameter space, as shown in Fig. 2.1, over which the dynamo is decaying when started with the weak field but produces a strong oscillatory field when started with a strong field. Overall the dynamo shows a hysteresis behaviour. This behaviour and the subcritical dynamo, was discovered in a simple mean-field dynamo with distributed α (Kitchatinov & Olemskoy, 2010). Later dynamo hysteresis was confirmed in magnetohydrodynamics (MHD) simulations of the helical turbulent dynamo with imposed shear (Karak et al., 2015b). Recently this was also seen in numerical simulations of turbulent α^2 dynamo (Oliveira et al., 2021).

As discussed in Kitchatinov & Olemskoy (2010), the imposed magnetic-field dependent nonlinearity in turbulent diffusivity and α makes the behaviour of the effective dynamo number $D_{\rm eff} = \alpha_0\phi_\alpha(\beta)\Omega R^3/\eta_0^2\phi_\eta(\beta)^2$ non-monotonic. When the magnetic field is large ($\beta \gg 1$), $D_{\rm eff}$ decreases with the increase of β ($D_{\rm eff} \sim \beta^{-1}$). In contrast, when β is small ($\beta \ll 1$), $D_{\rm eff}$ increases with the increase of β ($D_{\rm eff} \sim D(1 + 16\beta^2/7)$); see Fig. 1 of Kitchatinov & Olemskoy (2010). Thus, when the simulation is started with a very weak field, $D_{\rm eff}$ remains small and cannot trigger the dynamo, making it subcritical. On the other hand, when the simulation is started with a strong field ($\beta \sim 1$), $D_{\rm eff}$ becomes large enough to produce dynamo action.

The time-latitude distributions of the toroidal magnetic fields from a simulation at critical $\alpha_0 = 28.10$ m s^{-1} (started with a weak field) and from a subcritical case at $\alpha_0 = 23$ m s^{-1}(started with a strong initial field) are shown in Fig. 2.2. We observe regular polarity reversal and some migration towards the equator. The cycle period is much shorter than the solar value. This short cycle is due to our chosen value of η_0 (= $5 \times 10^{12} cms^2$). The high diffusivity always tends to produce short cycle (Karak & Choudhuri, 2012; Karak & Cameron, 2016) unless we reduce the diffusivity at BCZ drastically and/or include a strong downward magnetic pumping (Kitchatinov & Olemskoy, 2012a; Karak & Cameron, 2016). In fact, if we do not include the nonlinearity in diffusivity, then the cycle

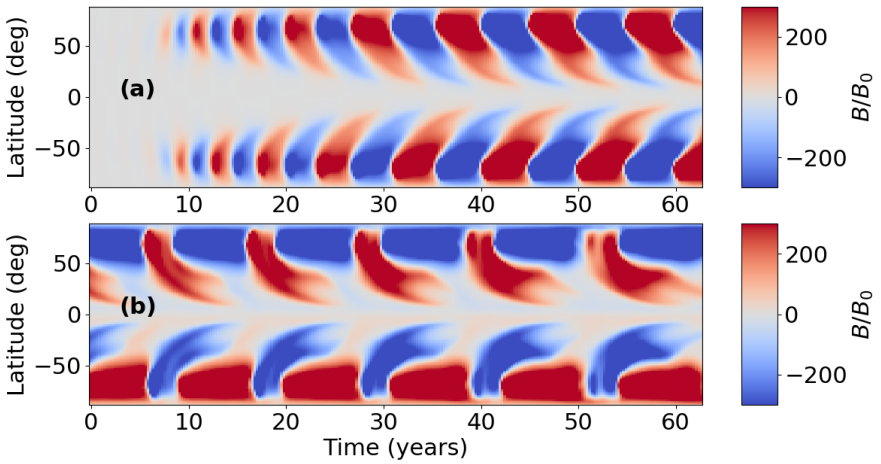

Figure 2.2: (a) Time-latitude distribution of the toroidal field at BCZ from a dynamo simulation at critical dynamo case ($\alpha = 28.10$ m s^{-1}) for which the simulation started with a weak field. (b) Same as (a) but from a subcritical dynamo case ($\alpha = 23$ m s^{-1}) and the simulation started with a strong field.

period is even shorter (~ 0.83 years).

One aspect of all these simulations is that they produce an unexpectedly strong magnetic field near the BCZ. In Fig. 2.1 and Fig. 2.2, we observe that the magnetic field strength is several tens of stronger than B_0. This strong field is caused by the strongly quenched diffusivity near the BCZ. We recall from Eq. (2.3)eq:etaqu that $\alpha_{\rm BL}$ and $\eta_{\rm T}$ are related to magnetic field locally. Near the BCZ, the magnetic field is usually stronger than that near the surface and thus at the BCZ, $\eta_{\rm T}$ is reduced strongly, but $\alpha_{\rm BL}$ is zero there. Hence this strongly reduced diffusivity near the BCZ in our Babcock–Leighton type dynamo is causing this strong magnetic field. This strong magnetic field is indeed in agreement with the super-equipartition field which was a prediction of the thin flux-tube simulations (D'Silva & Choudhuri, 1993; Caligari et al., 1995).

2.3.2 Quenching with the non-local field

Regular dynamo solutions and hysteresis

The Babcock–Leighton α is a nonlocal process in which the magnetic field at the BCZ acts as the seed for the poloidal field; see Eq. (2.2). Therefore, instead of connecting $\alpha_{\rm BL}$ and $\eta_{\rm T}$ with the local magnetic field, we now connect them with the magnetic field at the BCZ, i.e.,

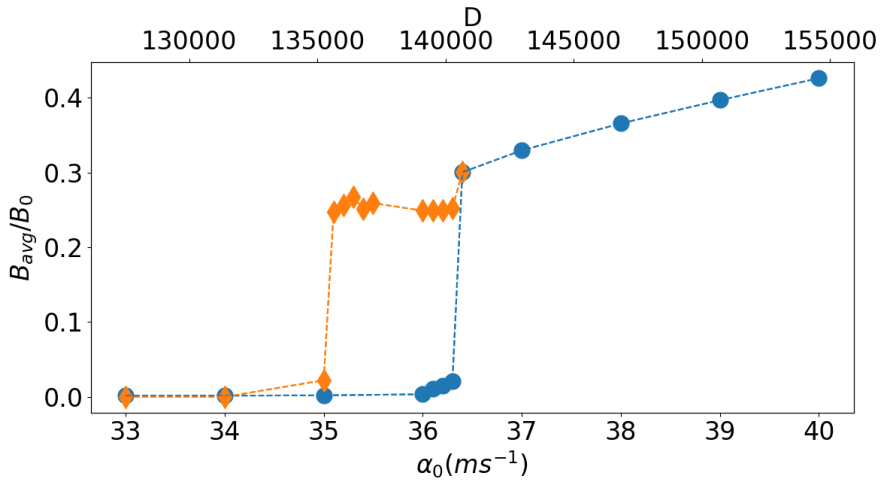

Figure 2.3: Same as Fig. 2.1 but obtained from simulations in which $\alpha_{\rm BL}$ and η_T are related to the toroidal field at the BCZ.

$$\alpha_{\rm BL} = \alpha\phi_\alpha(\overline{\beta}), \quad \eta_T = \eta\phi_\eta(\overline{\beta}), \tag{2.9}$$

where $\overline{\beta} = \overline{B}/B_0$. The quenching functions ϕ_α and ϕ_η will be computed from the same equations (2.5) and (2.8) but based on the average toroidal field at BCZ ($\overline{B}$). No other changes are made in the model.

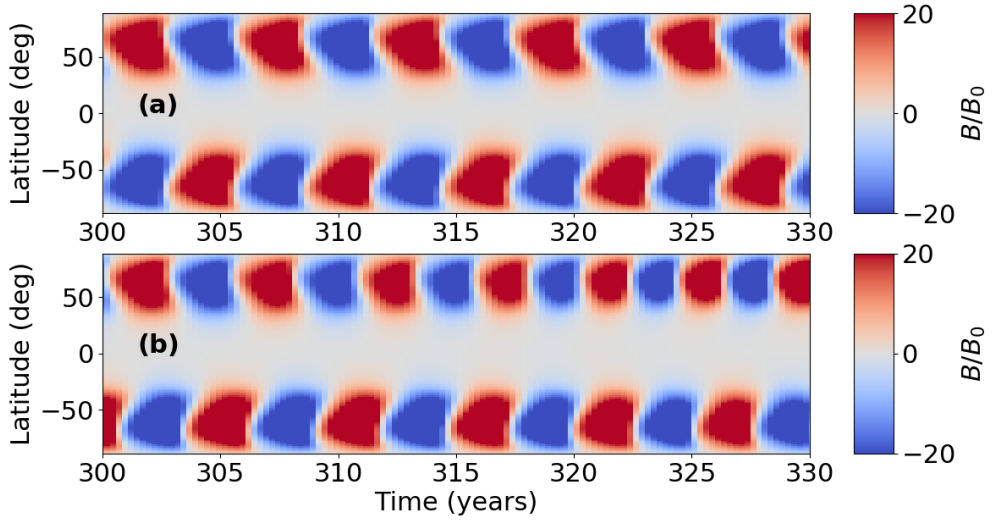

Figure 2.4: Butterfly diagrams for (a) toroidal field at BCZ for critical dynamo for the case ($\alpha_0 = 36.40$ m s^{-1}) when the simulation started with a weak magnetic field and (b) for subcritical dynamo case ($\alpha_0 = 35$ m s^{-1}) and started with the output of a strong oscillatory solution at $\alpha_0 = 36$ m s^{-1}.

We perform the simulations at different values of α_0 in the same way as we have done to produce Fig. 2.1. Fig. 2.3, shows the results. We immediately notice that the magnetic field strength is reduced, at least by an order of magnitude. We again find a regime in

the dynamo parameter where two solutions are possible: a weak decaying field and a strong oscillatory field, depending on the initial condition. Thus, the dynamo hysteresis is a generic feature in the Babcock–Leighton type solar dynamo.

Fig. 2.4 shows the time-latitude distribution of the toroidal field from simulation at the critical $\alpha_0 = 36.40$ m s^{-1}(started with a weak field) and at the subcritical dynamo, $\alpha_0 = 35$ m s^{-1}(started with a strong oscillating field). Although we see some general features of the solar magnetic field in this simulation, the cycle period is considerably reduced. The average period of the magnetic field oscillation is about 2.5 years. This short cycle period is due to different nonlinear quenching in α and η. Further, the field is strongest near the poles.

Dynamo with fluctuations in α

So far in each simulation, all dynamo parameters were kept constant and thus the non-linearity in our model kept the amplitude of the magnetic cycle nearly equal. However, due to fluctuating nature of the stellar convection, the dynamo parameter, especially the α is subjected to fluctuate around its mean. In the Babcock–Leighton scenario, the fluctuations are primarily seen in the form of scatter in the bipolar active region tilts around Joy's law (e.g., Stenflo & Kosovichev, 2012; Jiang et al., 2014b; McClintock et al., 2014; Wang et al., 2015; Arlt et al., 2016; Jha et al., 2020) and the randomness in flux emergence (Karak & Miesch, 2017). On the other hand, in the turbulent mean-field α, the scatter is unavoidable due to finite numbers of convection cells (Choudhuri, 1992). The fluctuations in α cause the polar field to change and thus make the magnetic cycle unequal as observed in sun and sun-like stars. This has been already used in many studies for modeling the irregular aspects of solar cycles (e.g., Charbonneau & Dikpati, 2000; Choudhuri et al., 2007; Choudhuri & Karak, 2009; Karak & Choudhuri, 2011; Olemskoy & Kitchatinov, 2013; Karak et al., 2018b).

Motivated by this, we include fluctuations in our Babcock–Leighton α. To do so, we replace α_0 by $\alpha_0 = \alpha_0[1 + s(\tau_{\rm corr}) \times f]$, where s is the uniform random number in the interval $-1 < s < 1$ and $\tau_{\rm corr}$ is the coherence time, which is taken as one month—

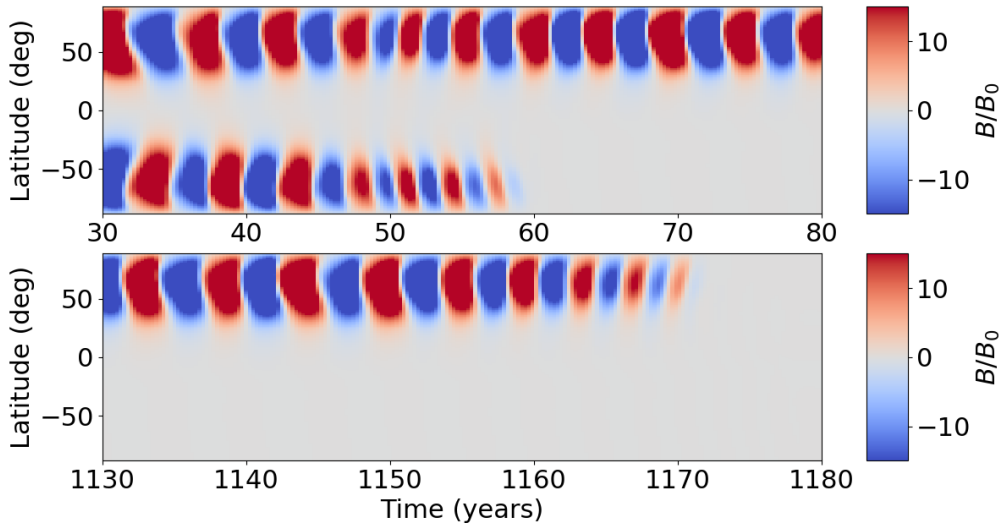

Figure 2.5: Butterfly diagrams of toroidal field for subcritical dynamo at $\alpha_0 = 35$ m s^{-1} with 20 percent fluctuations. Note that the duration 80–1130 years, i.e., the time spans shown in between two panels are not displayed.

consistent with the mean lifetime of BMRs. Thus, now in our model, the value of α_0 is updated randomly every one month. The level of fluctuations is determined by f. For example, $f = 1$, and 0.2 correspond to 100% and 20% fluctuations, respectively.

We find that for subcritical and slightly above critical regimes, this model tends to decay at large fluctuations. The dynamo dies even at 10% fluctuations. Fig. 2.5 shows the butterfly diagram of a subcritical dynamo ($\alpha_0 = 35$ m s^{-1}) in which the magnetic field decayed after about 1000 years due to large fluctuations. We note that this did not happen simultaneously in two hemispheres. Thus the subcritical branch is unstable under the large fluctuations. We have checked that if the fluctuation level is below 10%, then the dynamo does not decay immediately; sometimes it decays in a few years and sometimes it produces cycles for thousands of years before the decay. This is surprising. However, this problem might be solved by adding a distributed α_0 in the CZ which has been a way for recovering the dynamo from a grand minimum (Karak & Choudhuri, 2013; Hazra et al., 2014).
However, in the supercritical regime, the dynamo maintains a stable solution even at a very large fluctuations. We observe that when we have included 20% fluctuations, subcritical and critical cases die whereas supercritical case $\alpha_0 = 40$ m s^{-1}survives. Hence, the critical dynamo number increases with the increase of the level of fluctuations.

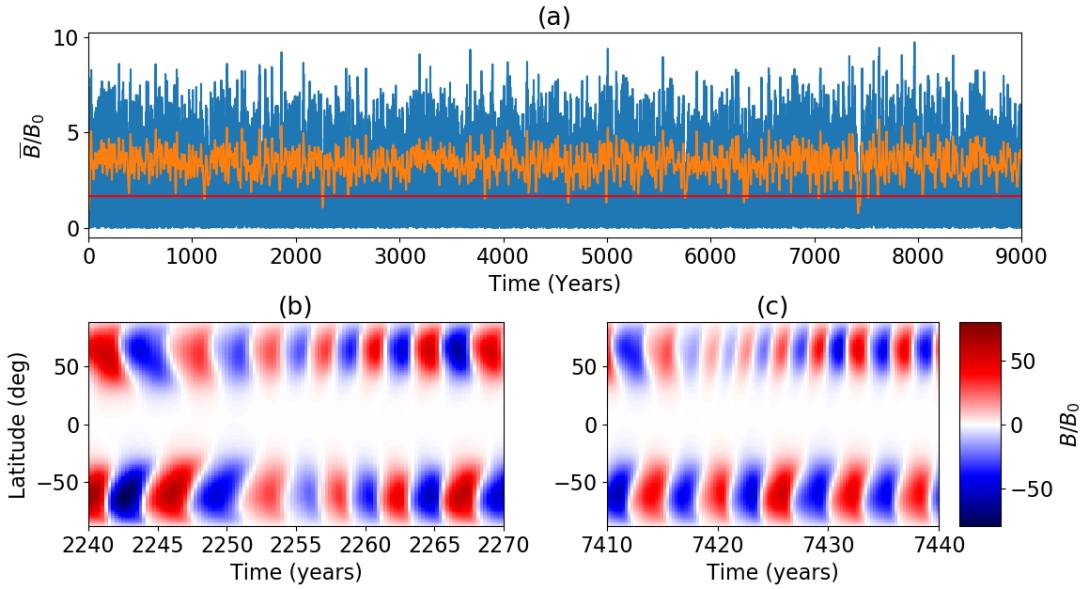

Figure 2.6: (a) Time series plot along with its smoothed curve (yellow) of toroidal magnetic flux. Red horizontal line shows the half of the mean of this smooth curve. (b) & (c) Butterfly diagram of toroidal field for the two grand minima. These are obtained from a supercritical dynamo at $\alpha_0 = 40$ m s^{-1}

The time series of the toroidal magnetic flux $\overline{B}$ at the BCZ from a simulation for 9000 years at $\alpha_0 = 40$ m s^{-1} is shown in Fig. 2.6(a). $\overline{B}$ is computed in a small region with $r = 0.677R_s$–$0.726R_s$ and latitudes: 10°–45°. We can see that the cycles are now variable, occasionally producing significantly strong and weak cycles. To check whether this simulation produces any grand minima or not, we apply the same method as performed in Usoskin et al. (2007) for the Sun. We bin the data for the duration of one cycle period (which is about 2.5 years in this simulation), filter the data by using Gleissberg's low-pass filter 1-2-2-2-1, and finally, count a grand minimum if this smoothed data falls below 50% of its mean for at least two cycle periods, which is 5 years in our case. In this way, we detect 6 grand minima. Two of such cases are presented in Fig. 2.6(b) and (c).

When we increase the supercriticality of the model by increasing α_0, the number of grand minima decreases. When $\alpha_0 \geq 42$ m s^{-1} we do not observe any grand minima. This is in some way in agreement with the stellar observations because only slowly rotating stars produce grand minima Baliunas et al. (1995), and the slowly rotating stars are expected to have a smaller value of α_0. This is because the efficiency of the Babcock–Leighton process depends on the tilt which is rooted to the rotation of the star (D'Silva & Choudhuri, 1993).

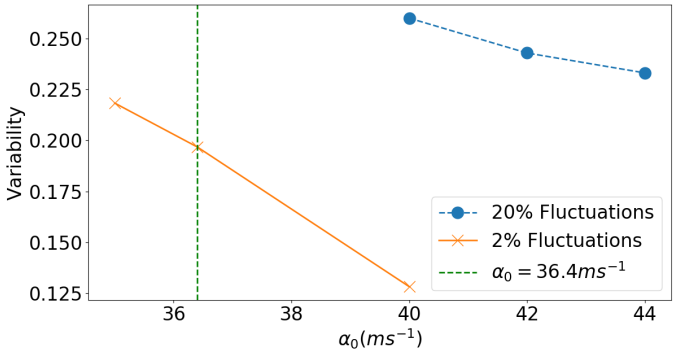

Figure 2.7: Variation of variability with respect to the increase in α_0 with 2% fluctuations (orange solid line) and with 20% fluctuations (blue dashed line).

The amount of variability of the cycle is obviously more when the fluctuation is more; see Fig. 2.7. To compute the variability, we first compute the peaks of the cycles as measured from the toroidal magnetic field time series $\overline{B}$. Then the root mean-square of the peaks divided by the mean is taken as the variability. The variability decreases with the increase of supercriticality of the model (α_0).

2.4 Conclusions

In this work, we have applied an axisymmetric kinematic dynamo model with a Babcock–Leighton $\alpha_{\rm BL}$ as the source of the poloidal field to explore the subcritical dynamo and the hysteresis behavior. We have included magnetic field-dependent nonlinearities in the $\alpha_{\rm BL}$ and diffusivity η_T based on the quasi-linear approximation (Ruediger & Kichatinov, 1993; Kitchatinov et al., 1994a). We have included these nonlinearities in two ways. First, we connect the $\alpha_{\rm BL}$ and η_T with the local toroidal magnetic field and then, we connect these with the toroidal field at the BCZ. We find regular polarity reversals and cycles if the dynamo number is above a critical value. We find a regime in the dynamo parameter where two solutions are possible: a weak decaying field and a strong oscillatory field, depending on the initial condition. Hence, the dynamo hysteresis, which was predicted in the distributed $\alpha\ \Omega$ dynamo (Kitchatinov & Olemskoy, 2010) and turbulent dynamo simulations (Karak et al., 2015b), also survives in Babcock–Leighton type dynamos. Thus, our study, along with previous studies, provides a possible existence of subcritical dynamo for executing large-scale magnetic cycles in sun-like stars.

By including stochastic fluctuations in $\alpha_{\rm BL}$, we check the stability of these subcritical branches. We find that when $\alpha_{\rm BL}$ and η_T are connected with the local magnetic field, the

subcritical branch maintains stable magnetic cycles. However, in the other case, when the $\alpha_{\rm BL}$ and η_T are connected with the magnetic field at the BCZ, the subcritical branch tends to decay with fluctuations. The supercritical branch is always stable and produces some grand minima. The number of grand minima and the cycle variability decrease with the increase of supercriticality (as controlled by the strength of $\alpha_{\rm BL}$ in our case).